Direct Measurements and Numerical Predictions of Welding-Induced Initial Deformations in a Full-Scale Steel Stiffened Plate Structure

Myung Su Yi[a], Dong Hun Lee[a], Hyun Ho Lee[a] and Jeom Kee Paik[a,b,c*]

[a]Department of Naval Architecture and Ocean Engineering, Pusan National University, Busan, Republic of Korea
[b]The Korea Ship and Offshore Research Institute (The Lloyd's Register Foundation Research Centre of Excellence), Pusan National University, Busan, Republic of Korea
[c]Department of Mechanical Engineering, University College London, London, UK
* Corresponding author. J.K. Paik. Email. j.paik@ucl.ac.uk

Abstract

As a sequel to another paper of the authors on welding-induced residual stresses [1], this paper aims to obtain a direct measurement database of welding-induced plate initial deflections in a full-scale steel stiffened plate structure and also to study the applicability of computational models to predict them. A full-scale steel stiffened plate structure in association with bottom plate panels of an as-built 1,900 TEU containership is fabricated by exactly the same technology of welding as used in today's shipbuilding industry. The 3D scanner is employed to measure welding-induced initial deformations of the structure. Computational models using the three-dimensional thermo-elastic-plastic finite element method are developed to predict the plate initial deflections. A comparison between direct measurements and numerical predictions is made. Details of direct measurement databases are documented as they are useful to validate the computational models formulated by other researchers.

Keywords: Steel stiffened plate structures, welding-induced initial deformations, full-scale measurements, three-dimensional thermo-elastic-plastic finite element method, 3D scanner

1. Introduction

Welding-induced initial deformations are unavoidable in fabrication of steel structures, as shown in Fig. 1, and they significantly affect the buckling and ultimate strength which are primary criteria for structural analysis and design [2,3]. Structural analysis and design need to start with an adequate definition of such initial imperfections. As would be expected, the welding-induced initial deformations in thin-walled structures are greater than in thick-walled structures. Thin-walled structures are likely to subject to thermal plate buckling in the process of fabrication, as shown in Fig. 2, resulting in costly fairing works to remove distortions.

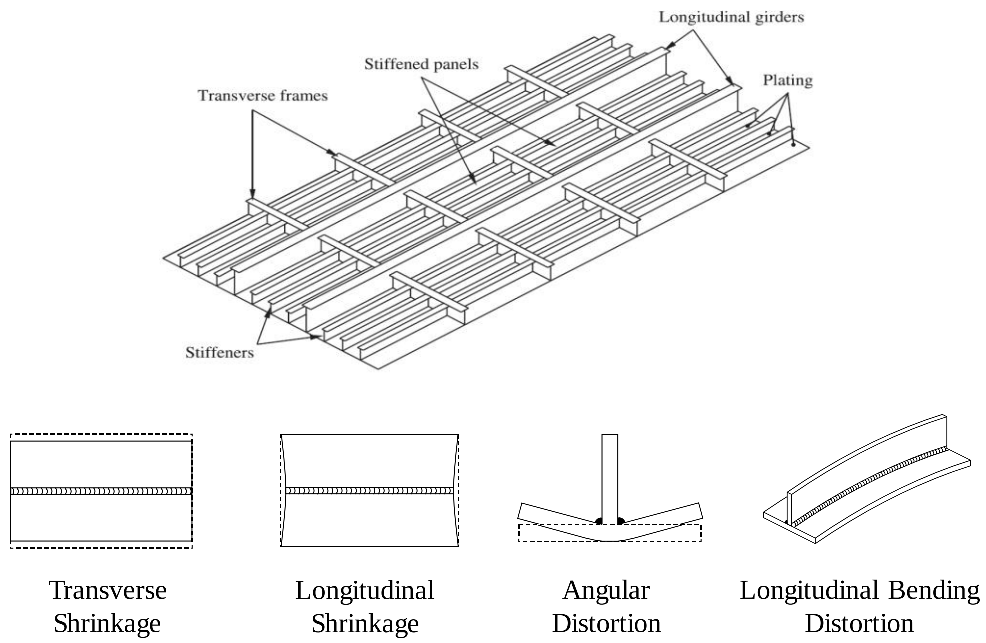

Fig. 1. Typical patterns of welding-induced initial deformations in stiffened plate structures [2].

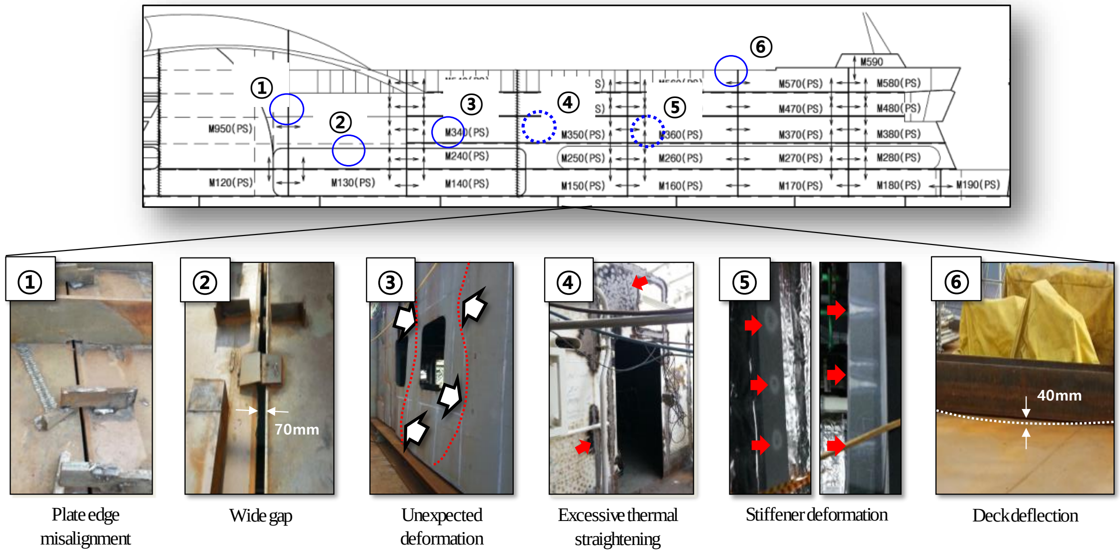

Fig. 2. Example of welding-induced deformations in thin-walled structures [5].

A number of studies on this topic are available in the literature, and their survey is found in Ueda [4] and Paik [2], among others. The previous studies include both direct measurements and numerical predictions. A few measurement studies were performed with full-scale structure models [5]. Most of previous studies used small-scale models which were far different from the actual welding in practice, which would significantly affect the resulting measured initial deformations in magnitude and pattern. Therefore, the development of direct measurement databases of welding-induced initial deformations in full-scale steel stiffened plate structures is highly demanded. A number of studies in numerical predictions of welding-induced initial deflections are also available in the literature [6-13].

The objective of the paper is to contribute to the development of direct measurement databases of welding-induced initial deformations in full-scale steel stiffened plate structures, and also to study the applicability of numerical predictions using the three-dimensional thermo-elastic-plastic finite element method models formulated by the authors [12,13]. This paper is a sequel to another article of the same authors on welding-induced residual stresses of a full-scale steel stiffened plate structure which is an identical structure used in the present paper [1].

2. Design of a full-scale steel stiffened plate structure model

In this paper, plate panels in bottom structures of an as-built containership carrying 1,900 TEU were chosen as the reference vessel, as shown in Fig. 3. Note that containerships in full load condition are in hogging and thus bottom plate panels are subjected to axial compressive loads [3,14,15].

Details of the scantlings for the test structure made of high tensile steel with grade AH32 are provided in Paik et al. [16], and a summary of the structural design is presented here. Fig. 4 shows the geometric properties the structure model which has T-type of longitudinal stiffeners and transverse frames as shown in Fig. 5. With the nomenclature of dimensions for longitudinal stiffeners and transverse frames, their geometric properties are provided in Table 1. The thickness of plating is 10 mm and the structure weighs 4.814 tons.

Fig. 3. Plate panels in bottom structures of an as-built 1,900 TEU containership.

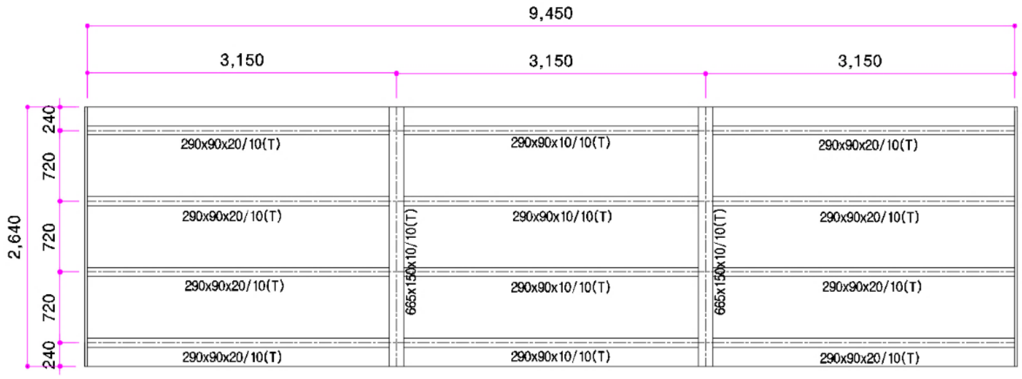

Fig. 4. Drawing of the full-scale steel stiffened plate structure.

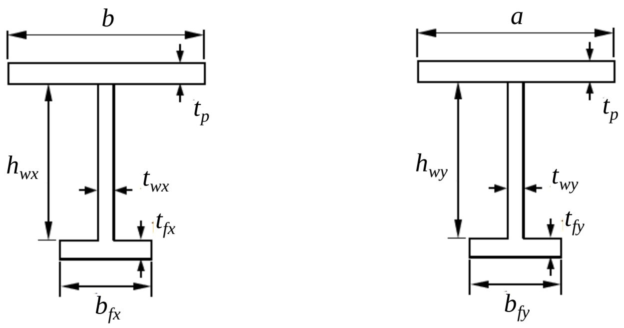

(a) Longitudinal stiffener (b) Transverse frame

Fig. 5. Nomenclature of dimensions.

Table 1. Dimensions of the structure model.

Plate properties			Stiffener / Frame properties					
Length, a (mm)	Breadth, b (mm)	Thickness, t_p (mm)	Type		h_w (mm)	t_w (mm)	b_f (mm)	t_f (mm)
3,150	720	10	Stiffener (T-bar type)	Center	290	10	90	10
				Both side	290	20	90	10
			Frame (T-bar type)	-	665	10	150	10

3. Fabrication of the structure model

The structure is made of high tensile steel with grade AH32. After the material procurement, tensile coupon test specimens were extracted from the steel sheet as per ASTM E8 [17], as shown in Fig. 6(a). The universal test machine together with an extensometer was used for the tension tests as shown in Fig. 6(b). The failure pattern of the tensile coupon specimens was similar, as shown in Fig. 6(c). Fig. 7 shows one of typical engineering stress-engineering strain curves of the material obtained from tensile coupon tests with multiple specimens. Table 2 provides the mechanical properties of material AH32.

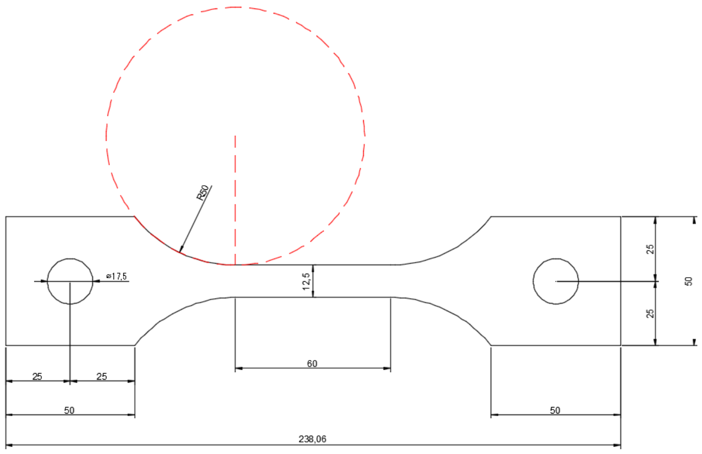

(a) Dimension of the tensile test specimen

(b) Specimen with extensometer (c) Specimen after completing tensile test

Fig. 6. Specimen of material used for the structure before and after tensile coupon tests.

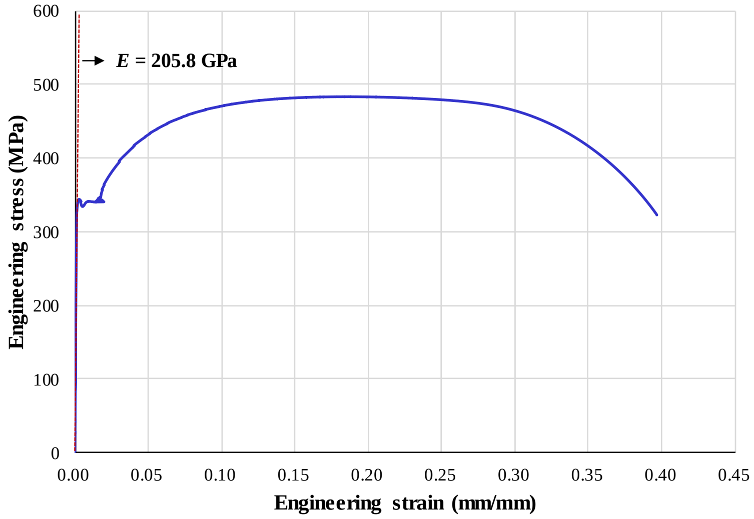

Fig. 7. Engineering stress versus engineering strain curve of material AH32.

Table 2. Mechanical properties of material AH32 used for the structure model.

Grade	E (GPa)	σ_Y (MPa)	σ_T (MPa)	ν	ε_f (%)
AH32	205.8	331	483	0.3	40.0

Note: E is the elastic modulus, σ_Y is the yield strength, σ_T is the ultimate tensile strength, ν is the assumed Poisson's ratio, and ε_f is the fracture strain.

Table 3. Welding parameters of the actual welding process and welding procedure specifications

L_w (mm)	Welding parameter				
		Current (A)	Voltage (V)	Speed (cm/min)	Heat input (KJ/cm)
7	WPS	225-275	23-32	24-34	7-18
	Real condition	260	28	30	14.56

The structure was fabricated in a shipyard in Busan, South Korea which builds small and medium sized merchant and patrol ships. The technology of welding was exactly the same as used for fabrication of real ship structures. The steel sheet was procured with one big plate to avoid butt welds to connect multiple pieces of plates. Support members (longitudinal stiffeners or transverse frames) are attached by fillet welds as per the welding requirements of DNVGL [18]. The flux-cored arc welding

(FCAW) technique was applied in accordance with the welding procedure specification (WPS) requirements as indicated in Table 3.

It is important to ensure whether the welding has been successful with full penetration of weld materials along weld lines. Fig. 8 confirms that the penetration of welding was fully achieved with a leg length of 7 mm. Fig. 9 shows photos of the structure after fabrication was completed in the shipyard.

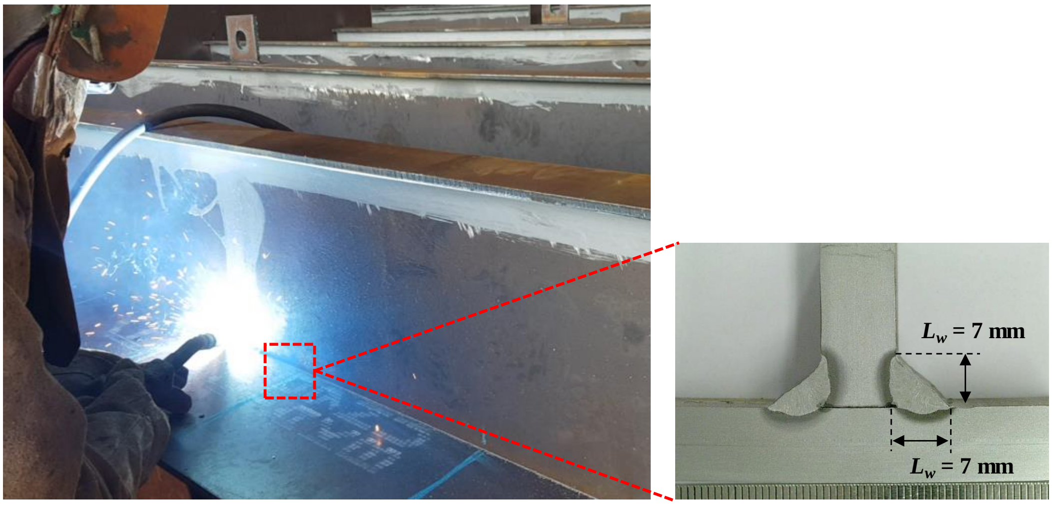

Fig. 8. Full penetration of welds with a leg length of 7 mmm.

Fig. 9. The structure after completing of fabrication in the shipyard.

4. Measuring methods of initial deformations

Three kinds of welding-induced initial deformations are relevant in stiffened plate panels, namely plate initial deflection, stiffener's deflection and sideways deformation. Appendix presents all of the three types of measured databases, but this section focuses on the measurements of plate initial deflection.

A 3D scanner as a non-contact method is employed to measure the welding-induced initial deformations. Table 4 provides the specifications of the 3D scanner used for the measurements. Details of the measuring methods using the 3D scanner may be referred to in Yi et al. [5]. Fig. 10 presents selective photos showing the measurements of initial deformations. As shown in Fig. 11, the measured data is automatically recorded by a personal computer in a digital form which can be easily converted for computational modeling. The measuring time was about 20 min. Appendix presents the details of measured databases in a tabulated form which can be used to validate computational models for predicting welding-induced initial deformations. Also, the measured databases are compared with numerical computations in the next section.

Table 4. Details of the 3D scanner used for the measurements.

	Measuring instrument : MetraSCAN750™	
	Accuracy	Up to 0.030 mm
	Resolution	0.050 mm
	Measurement rate	480,000 measurements/s
	Accurate measurement of part ranging	0.2 – 10 m
	Operating temperature	5 – 40 ℃

Fig. 10. Photos showing the measurements of the welding-induced initial deformations using 3D scanner

(a) Initiation of measuring points

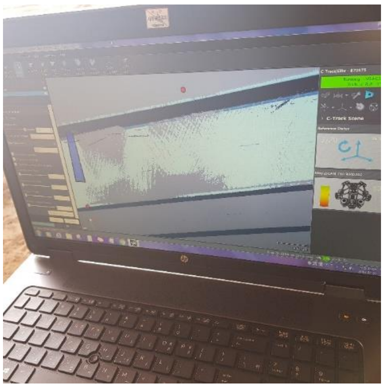

(b) Acquisition of scanned images

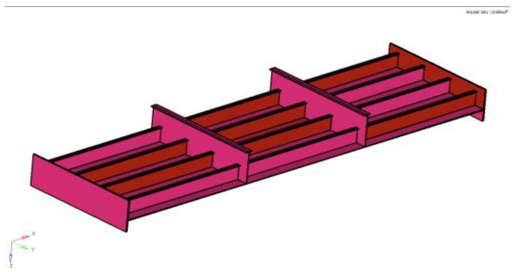

(c) Creating a space with scanned data

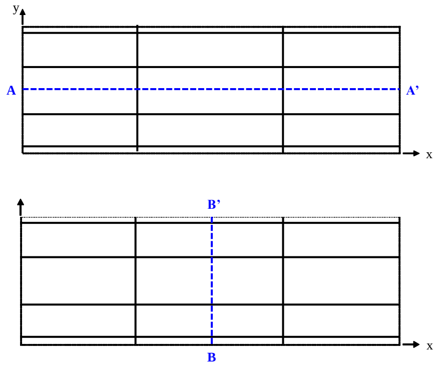

(d) Extraction of data of interest

Fig. 11. Process of measuring welding-induced initial deformations

5. Computational models using the thermo-elastic-plastic finite element method

The shape of welding-induced initial deformations in plate panels is very complex [4]. Thinner plate panels may show more complex patterns of initial deformations. The shape of welding-induced initial deformations in plate panels is often modeled as a combination of multiple sinusoidal waves [2,4,5], but an accurate prediction is sometimes required unless direct measurements are realistic.

In this paper, computational models are developed to predict welding-induced initial deformations of plate panels using three-dimensional thermo-elastic-plastic finite element method [12,13] and compared with measured data. As details of the computational modeling techniques are referred to in Seo et al. [12] and Yi et al. [13], only a brief description is made in this paper.

The computational modeling was created in three steps, as shown in Fig. 12. Step I performs a pre-initial deflection analysis where the strain-as-direct-boundary (SDB) technique is applied, which is recognized as one of simplified methods to predict welding-induced initial deformations [19,20]. In Step II, welding induced shrinkage forces (S.F.) are estimated from the relationship with effective heat (Q') input as shown in Fig. 13 [12,21]. In Step III, thermal buckling is analyzed with the pre-initial deflections and the shrinkage forces determined in Step II. All of the computations follow the thermo-elastic-plastic finite element method.

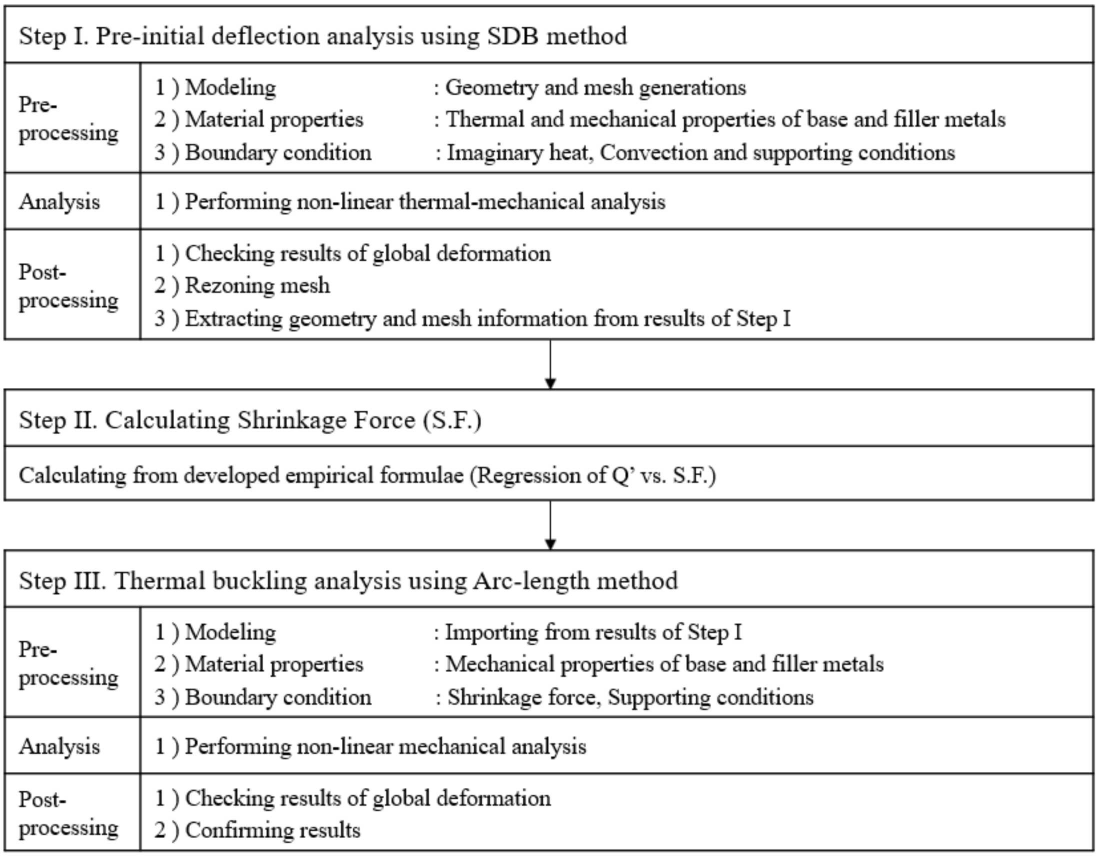

Fig. 12. Procedure for predicting welding-induced initial deflections in plate panels [12,13]

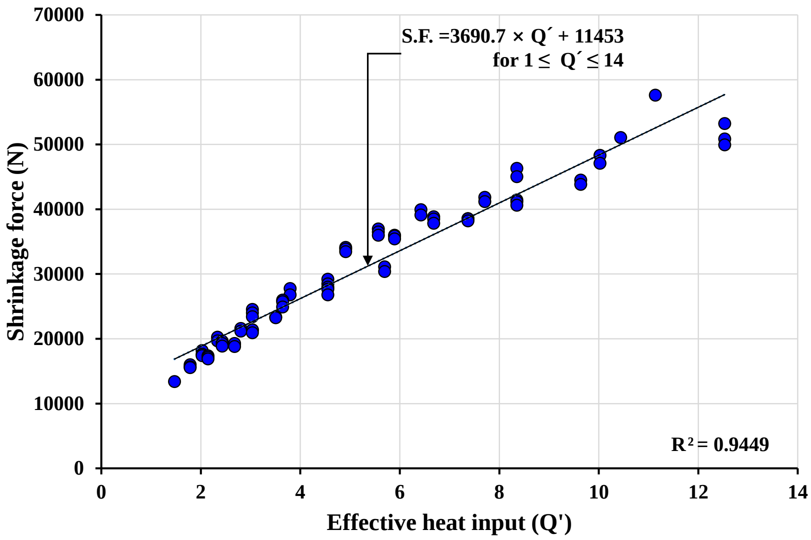

Fig. 13. Relationship between the shrinkage force versus the effective heat [12].

In the present study, the strain-hardening effects of material are not taken into account, while the mechanical properties of material as indicated in Table 2 are used. The geometry of plate panels is modelled by rectangular type plate-shell finite elements, where the gradient of temperatures over the cross section in the plate thickness direction is approximately distributed.

The analysis of Step I reveals initial irregularities in the shape of plate panels, where spring elements are used with self-weight at the four vertices of the analysis model. All the six degrees of freedom at the nodes of these spring elements are constrained to prevent rigid body motion. To simulate the situation of an actual welding process, the contact analysis with structural elements is performed in un-deformed state. A contact-friction model is applied using a stick-slip modeling technique for efficient convergence. Fig. 14 presents the boundary conditions of the computational models where a symmetric condition is applied along all the four edges of plate panels. This condition is in fact not directly equivalent to the test structure which is a stand-alone plate panel, but it was adopted because real plate panels are arranged continuously in the middle of plated structures. Thermal loads in terms of temperatures at top and bottom surfaces of plating are obtained from the analyses of Steps I and II as indicated in Table 5 and they are then applied to individual finite elements along each welding line.

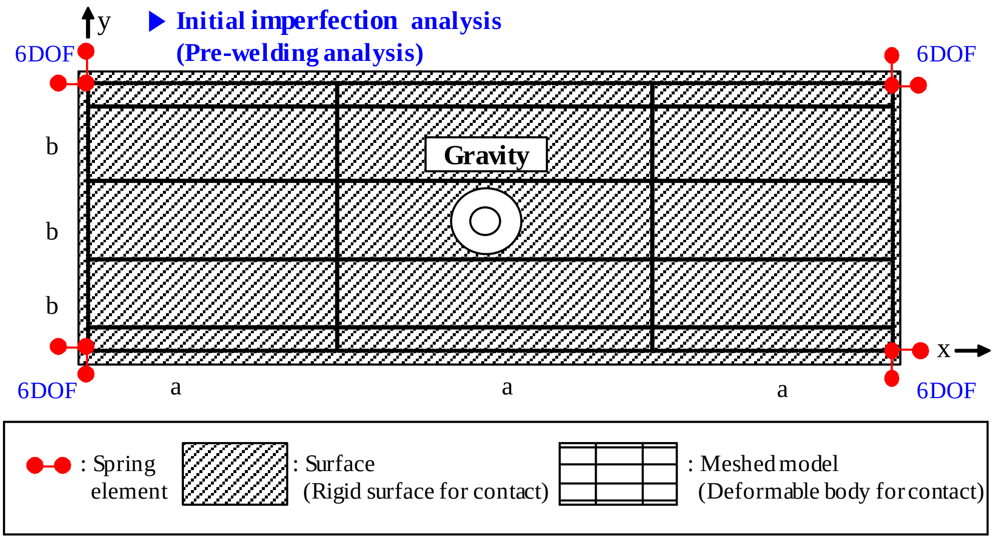

(a) Modelling for Step I analysis (prediction of initial irregularities)

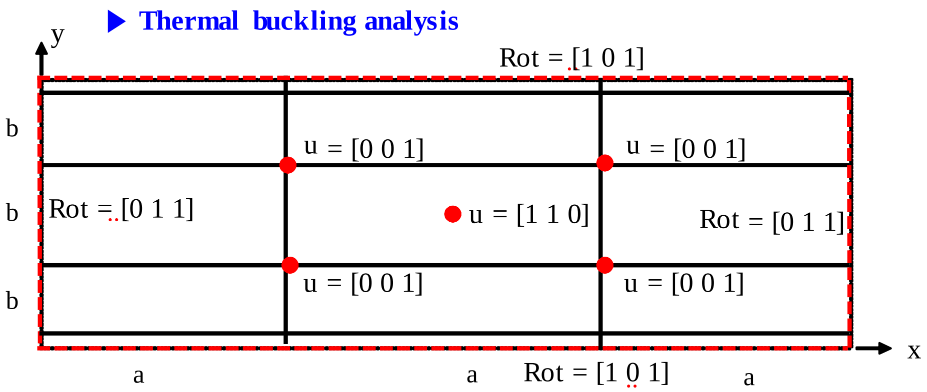

(b) Boundary condition for Step III analysis (thermal buckling analysis)

Fig. 14. Computational modelling for prediction of welding-induced initial deformations in the test structure.

Table 5. Shrinkage forces and temperatures obtained from Steps I and II.

t_p (mm)	L_w (mm)	S.F. (N)	Imaginary Temp. top, T_{top} (℃)	Imaginary Temp. bottom, T_{bot} (℃)
10	7	31,861.09	0.174	-0.174

Note. t_p = thickness of plating, L_w = leg length of welding, T_{top} = temperature at top surface of plating, T_{bot} = temperature at bottom surface of plating.

6. Results and Discussions

Fig. 15 presents the results of computational predictions for welding-induced initial deflections in the structure. Fig. 15 compares the direct measurements and numerical computations of plate initial deflections at cross sections A-A’ and B-B’ of the test structure.

It is seen from Fig.s 15 and 16 that plate initial deflections happened to one side, i.e., support member side of the structure. Not only plating but also transverse frames deflected by welding. During fabrication, four edges of the structure were left free without constraints. The resulting distortions are small along the short edges of the structure. However, the long edges of the structure were distorted unsymmetrically. The welding-induced initial deflections of plating between transverse frames shows the shape of so-called hungry horse’s back, and may be modeled as a combination of multiple sinusoidal waves [2].

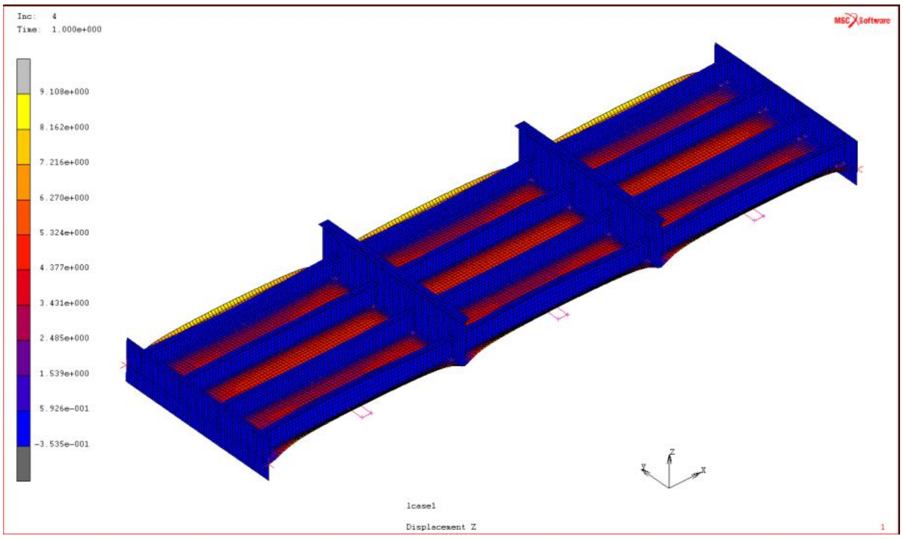

(a) Results of step I analysis.

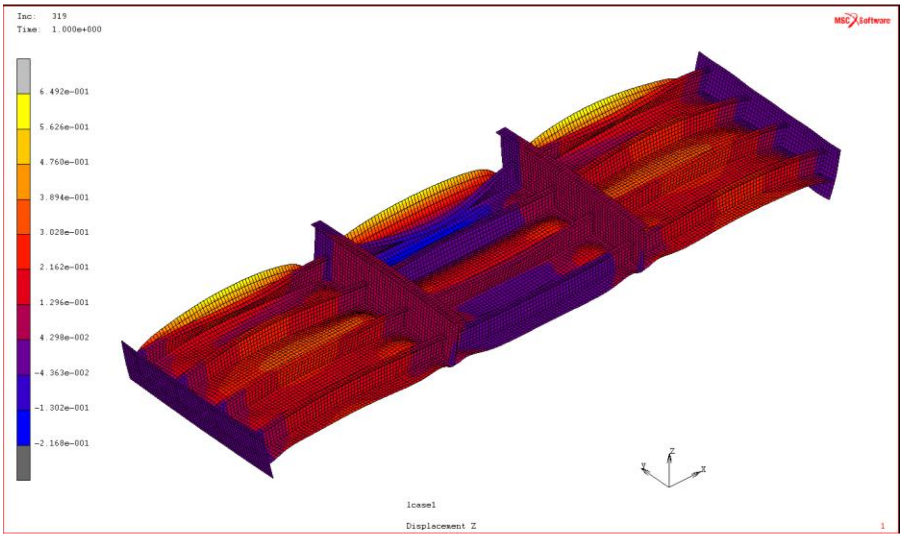

(b) Results of step III analysis.

Fig. 15. Results of the computational predictions.

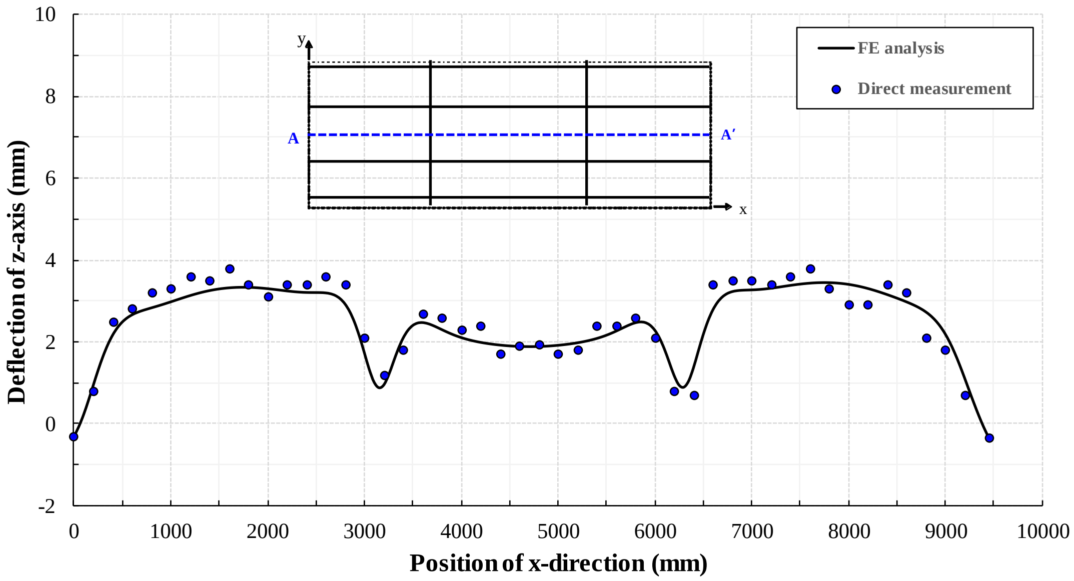

(a) Welding-induced initial deflection of plating in the plate length direction.

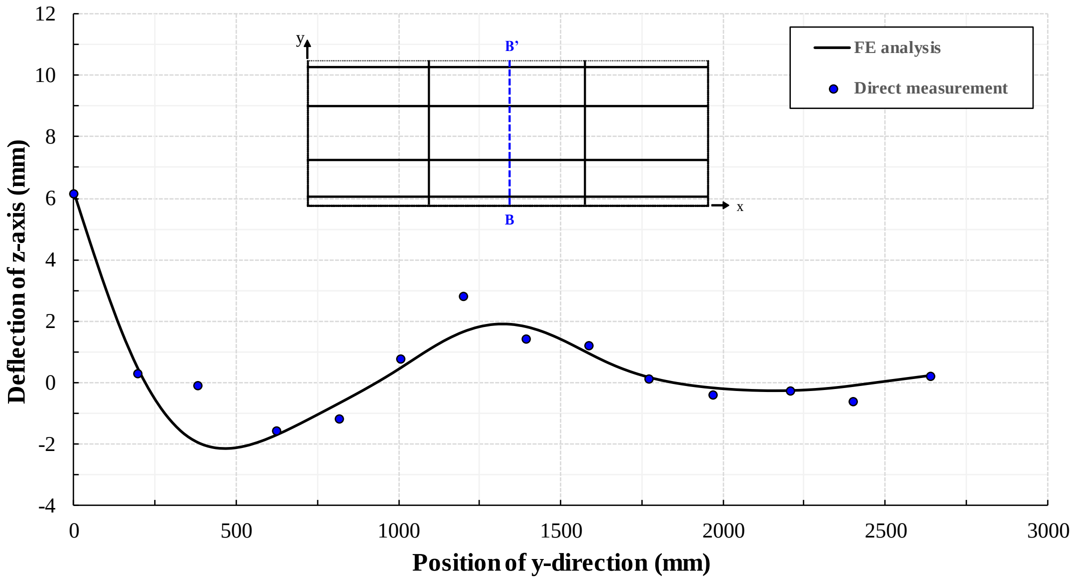

(b) Welding-induced initial deflection of plating in the plate breadth direction.

Fig. 16. Comparison between direct measurements and numerical computations of plate initial deflections in the test structure.

Fig. 17 shows the statistical error assessment between direct measurements and numerical computations in plate initial deflection. The mean value and standard deviation are 1.087 and 0.198, respectively in the plate length direction, and 0.890 and 0.391, respectively in the plate breadth direction.

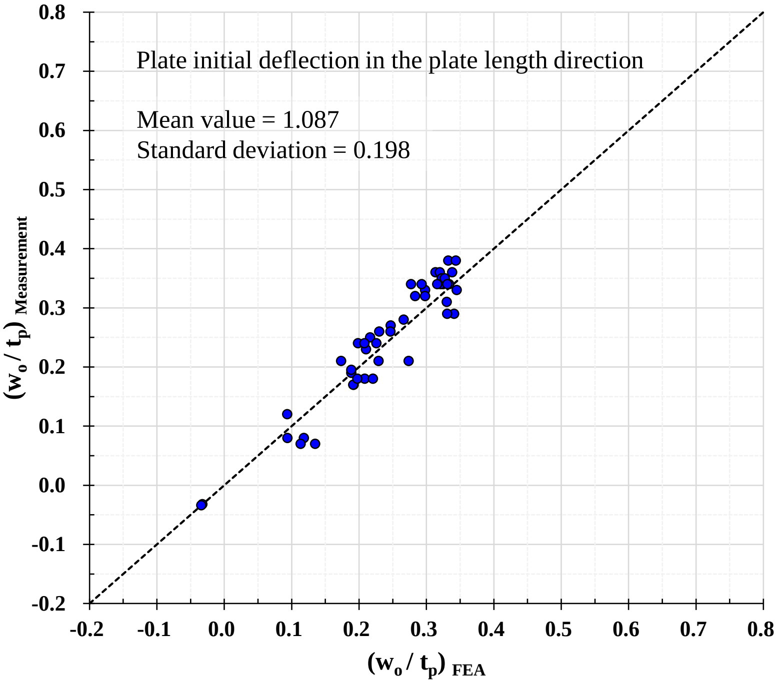

(a)

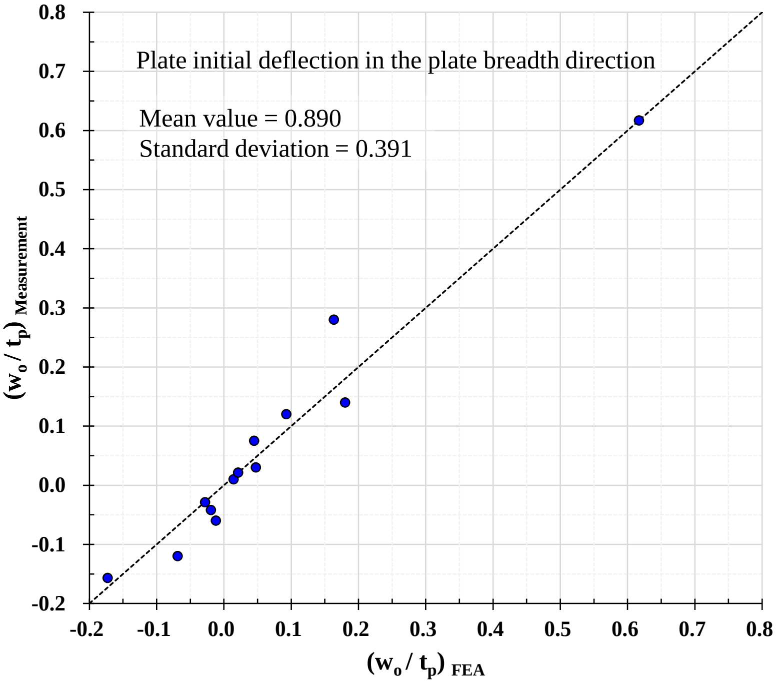

(b)

Fig. 17. Statistical analysis of the plate initial deflection: (a) plate length direction, (b) plate breadth direction.

Ship classification societies or other regulatory bodies specify construction tolerances for strength members as related to the maximum initial deflections with the intention that the initial deformations in the fabricated structure must be less than the corresponding specified values [2]. Some examples of the limit for the maximum plate initial deflections are as follows:

NORSOK [22]

$$\frac{w_{o\max}}{b} \le 0.01$$

Japanese shipbuilding quality standards [23]

$$w_{o\max} \le \begin{cases} 7\ mm\ \ for\ \ ship\ bottom\ \ plate \\ 6\ mm\ \ for\ \ ship\ deck\ \ plate \end{cases}$$

where $w_{o\max}$ is the maximum or limit of the plate initial deflection, and t is the plate thickness.

When the above equations of tolerance are applied to the test structure of this study, the following checks can be made.

In the plate length direction ($w_{o\max}$ = 3.80 mm),

$$\frac{w_{o\max}}{b} = \frac{3.80}{720} = 0.0053 \le 0.01$$

$$w_{o\max} = 3.80\ mm \le \begin{cases} 7\ mm\ \ for\ \ ship\ bottom\ \ plate \\ 6\ mm\ \ for\ \ ship\ deck\ \ plate \end{cases}$$

In the plate breadth direction ($w_{o\max}$ = 6.17 mm),

$$\frac{w_{o\max}}{b} = \frac{6.17}{720} = 0.0086 \le 0.01$$

$$w_{o\max} = 6.17\ mm \le \begin{cases} 7\ mm\ \ for\ \ ship\ bottom\ \ plate \\ 6\ mm\ \ for\ \ ship\ deck\ \ plate \end{cases}$$

For the stiffened-plate structure studied in the present paper, the welding-induced initial deflection satisfies the tolerance limit by ship classification societies or other regulatory bodies, confirming that the fabrication of the test structure was good enough.

7. Concluding remarks

The aim of the paper was to obtain direct measurement databases of welding-induced initial deflections in a full-scale steel plate structure, and also to compare them with computational predictions. Based on the study, the following conclusions can be drawn.

(1) A full-scale steel stiffened plate structure was designed and fabricated in a shipyard using exactly the same technology of welding as used in today's shipbuilding industry.

(2) 3D scanner was used for measuring welding-induced initial deflections of plate panels as a non-contact method. It is confirmed that the 3D scanner is useful to measure the welding-induced initial deformations.

(3) Three-dimensional thermo-elastic-plastic finite element method models were developed to predict welding-induced initial deformations of the structure. It is confirmed that the computational models predict the magnitude and shape welding-induced initial deflections of plate panels at a reasonable level of the accuracy.
(4) The database obtained in the paper will be useful for validating computational models developed by other engineers.

Acknowledgements

This work was conducted at the International Centre for Advanced Safety Studies / Korea Ship and Offshore Research Institute (www.icass.center) which has been a Lloyd's Register Foundation Research Centre of Excellence since 2008.

ORCID

Myung Su Yi. http://orcid.org/0000-0002-6984-5146
Dong Hun Lee. http://orcid.org/0000-0003-2829-0719
Hyun Ho Lee. http://orcid.org/0000-0001-7073-1069
Jeom Kee Paik. http://orcid.org/0000-0003-2956-9359

References

[1] M.S. Yi, S.H. Noh, D.H. Lee, D.H. Seo, J.K. Paik, Direct measurements, numerical predictions and simple formula estimations of welding-induced residual stresses in a full-scale steel stiffened plate structure, The Korea Ship and Offshore Research Institute, Pusan National University, Busan, South Korea, 2020.
[2] J.K. Paik, Ultimate Limit State Analysis and Design of Plated Structures, Second Edition, Chichester, UK, 2018.
[3] J.K. Paik, Advanced structural safety studies with extreme conditions and accidents, Springer, Singapore, 2019.
[4] Y. Ueda, Computational welding mechanics (selected from papers published in English), Joining and Welding Research Institute, Osaka University, Osaka, Japan, 1999.
[5] M.S. Yi, C.M. Hyun, J.K. Paik, Full-scale measurements of welding-induced initial imperfections in steel stiffened plate structures, International Journal of Maritime Engineering, Transactions of the Royal Institution of Naval Architects, 160(A4) (2018) 397-412.
[6] Y. Luo, D. Deng, L. Xie, H. Murakawa, Prediction of deformation for large welded structures based on inherent strain, Transactions of Joing and Welding Research Institute, Osaka University, Osaka, Japan, 33(1) (2004) 65-70.
[7] R. Wang, J. Zhang, H. Serizawa, H. Murakawa, Study of welding inherent defor-mations in thin plates based on finite analysis using interactive substructure method, Materials & Design, 30(9) (2009) 3474-3481.
[8] D. Deng, H. Murakawa, W. Liang, Numerical simulation of welding distortion in large structures, Comput Methods Appl Mech Eng. 196(45-48) (2007) 4613-4627.

[9] T. Gray, D. Camilleri, N. McPherson, Control of welding distortion in thin-Plate fab-rication: design support exploiting computational simulation, England Cambridge: Woodhead Publishing Limited. 2014.
[10] F. Guangming, I.L. Marcelo, D. Menglan, F.E. Segen, Influence of the welding sequence on residual stress and distortion of fillet welded structures, Marine Structures. 46 (2016) 30-55.
[11] J. Wang, H. Yuan, N. Ma, H. Murakawa, Recent research on welding distortion pre-diction in thin plate fabrication by means of elastic FE computation, Marine Structures, 47 (2016) 42-59.
[12] J.K. Seo, M.S. Yi, S.H. Kim, B.J. Kim, S.J. Kim, Welding distortion design formulae of thin-plate panel structure during the assembly process, Ships and Offshore Structures, 13(S1) (2018) 364-377.
[13] M.S. Yi, C.M. Hyun, J.K. Paik, Three-dimensional thermo-elastic-plastic finite element method modelling for prediction weld-induced residual stresses and distortions in steel stiffened-plate structures, World Journal of Engineering and Technology, 6 (2018) 176-200.
[14] O.F. Hughes, J.K. Paik, Ship structural analysis and design, Alexandria, USA: The Society of Naval Architects and Marine Engineers, 2013.
[15] J.K. Paik, D.H. Lee, S.J. Kim, G. Thomas, M. Ma, A new method for determining the design values of wave-induced hull girder loads acting on ships, Ships and Offshore Structures, 14(S1) (2019) S63-S90.
[16] J.K. Paik, D.H. Lee, S.H. Noh, D.K. Park, J.W. Ringsberg, A full-scale physical model testing on the ultimate limit states of a steel stiffened plate structure under cyclic compressive loading, Submitted for publication, 2019.
[17] ASTM, ASTM E8/E8M-09 Standard test methods for tension testing of metallic materials, PA, USA: American Association State International, 2011.
[18] DNVGL, Rules for classification – ships, Part 2 Materials and welding, Chapter 4 Fabrication and testing, Høvik, Norway, 2017.
[19] Y.S. Ha, S.H. Cho, T.W. Jang, Development of welding distortion analysis method using residual strain as boundary condition, Material Science Forum, (2008) 649-654.
[20] Y.S. Ha, A study on weldment boundary condition for elasto-plastic thermal distortion analysis of large welded structures, Journal of Welding and Joining. 29(4) (2011) 410-415.
[21] D.J. Lee, S.B. Shin, A study on the prediction of shrinkage during the manufacturing of a deckhouse of RIG, Proceedings of International Offshore and Polar Engineering Conference, (2003) 166-171.
[22] NORSOK, Design of steel structures, N-004, Rev.2, Standards Norway, Lysaker, Norway, 2004.
[23] JSQS, Japanese shipbuilding quality standards, The Society of Naval Architects of Japan, Tokyo, Japan, 1985.

Appendix: Measured welding-induced initial deformations of the test structure

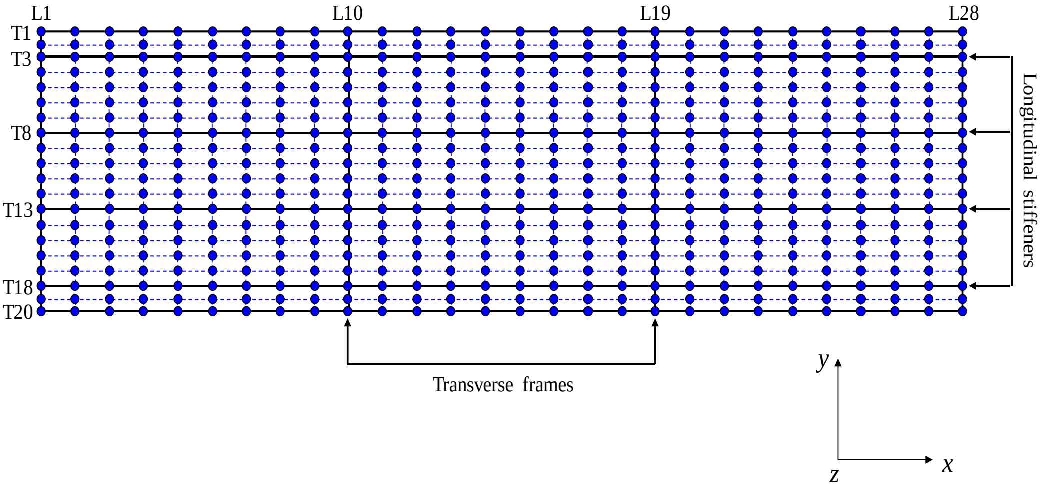

Fig. A.1. Measurement locations.

Table A1. Measured database of the initial deflections normalized by plate thickness

(a) Plate initial deflection for a = 0 ~ 3,150 mm (z-direction)

Plate initial deflections (w_0 / t_p)			Longitudinal direction (a = 0 ~ 3,150 mm)									
			0	350	700	1,050	1,400	1,750	2,100	2,450	2,800	3,150
			L1	L2	L3	L4	L5	L6	L7	L8	L9	L10
Transverse direction (b = 0 ~ 2,640 mm)	0	T1	-0.00033	0.01476	0.01891	0.02164	0.02286	0.02172	0.01834	0.01422	0.01532	0.00307
	120	T2	-0.00072	0.01097	0.01674	0.02024	0.02147	0.02052	0.01772	0.01376	0.01153	0.00519
	240	T3	-0.00110	0.00904	0.01565	0.01918	0.02027	0.01946	0.01726	0.01409	0.01024	0.00616
	384	T4	-0.00154	0.01159	0.01678	0.01843	0.01899	0.01837	0.01727	0.01732	0.01689	0.00719
	528	T5	-0.00198	0.01561	0.01912	0.01856	0.01861	0.01812	0.01792	0.02134	0.02566	0.00792
	672	T6	-0.00238	0.01585	0.01932	0.01895	0.01915	0.01863	0.01825	0.02154	0.02663	0.00845
	816	T7	-0.00272	0.01179	0.01729	0.01966	0.02066	0.02001	0.01847	0.01802	0.01887	0.00879
	960	T8	-0.00301	0.00878	0.01694	0.02170	0.02354	0.02298	0.02056	0.01690	0.01272	0.00895
	1,104	T9	-0.00313	0.01316	0.02157	0.02583	0.02811	0.02817	0.02635	0.02338	0.01917	0.00895
	1,248	T10	-0.00322	0.01858	0.02685	0.02964	0.03200	0.03274	0.03199	0.03102	0.02805	0.00881
	1,392	T11	-0.00322	0.01868	0.02698	0.02984	0.03222	0.03292	0.03211	0.03111	0.02827	0.00854
	1,536	T12	-0.00315	0.01331	0.02177	0.02612	0.02837	0.02832	0.02634	0.02330	0.01930	0.00814
	1,680	T13	-0.00305	0.00880	0.01685	0.02141	0.02300	0.02218	0.01956	0.01578	0.01154	0.00760

	1,824	T14	-0.00275	0.01195	0.01675	0.01813	0.01839	0.01733	0.01562	0.01475	0.01485	0.00702
	1,968	T15	-0.00242	0.01604	0.01779	0.01538	0.01416	0.01294	0.01234	0.01504	0.01991	0.00628
	2,112	T16	-0.00202	0.01540	0.01631	0.01309	0.01124	0.00963	0.00897	0.01208	0.01804	0.00545
	2,256	T17	-0.00157	0.01108	0.01414	0.01372	0.01258	0.01064	0.00867	0.00852	0.01051	0.00453
	2,400	T18	-0.00112	0.01030	0.01773	0.02154	0.02233	0.02073	0.01738	0.01293	0.00803	0.00346
	2,520	T19	-0.00073	0.01605	0.02597	0.03217	0.03474	0.03410	0.03063	0.02445	0.01567	0.00269
	2,640	T20	-0.00033	0.02617	0.03901	0.04751	0.05223	0.05329	0.05072	0.04391	0.03108	0.00155

(b) Plate initial deflection for a = 3,150 ~ 6,300 mm (z-direction)

Plate initial deflections (w_0 / t_p)			Longitudinal direction (a = 3,150 ~ 6,300 mm)									
			3,150	3,500	3,850	4,200	4,550	4,900	5,250	5,600	5,950	6,300
			L10	L11	L12	L13	L14	L15	L16	L17	L18	L19
Transverse direction (b = 0 ~ 2,640 mm)	0	T1	0.00307	0.00870	0.00175	0.00117	0.00145	0.00140	0.00104	0.00158	0.00860	0.00312
	120	T2	0.00519	0.00495	0.00126	0.00047	0.00018	0.00013	0.00036	0.00112	0.00487	0.00527
	240	T3	0.00616	0.00367	0.00154	-0.00014	-0.00106	-0.00110	-0.00025	0.00140	0.00360	0.00626
	384	T4	0.00719	0.01029	0.00465	-0.00030	-0.00235	-0.00238	-0.00039	0.00455	0.01024	0.00729
	528	T5	0.00792	0.01900	0.00870	0.00043	-0.00250	-0.00252	0.00036	0.00863	0.01899	0.00803
	672	T6	0.00845	0.02001	0.00911	0.00106	-0.00164	-0.00166	0.00102	0.00908	0.02006	0.00856
	816	T7	0.00879	0.01253	0.00603	0.00186	0.00043	0.00042	0.00184	0.00603	0.01259	0.00891
	960	T8	0.00895	0.00682	0.00563	0.00500	0.00473	0.00473	0.00501	0.00566	0.00688	0.00907
	1,104	T9	0.00895	0.01373	0.01304	0.01227	0.01196	0.01198	0.01232	0.01312	0.01380	0.00907
	1,248	T10	0.00881	0.02277	0.02133	0.01898	0.01812	0.01815	0.01907	0.02146	0.02289	0.00892
	1,392	T11	0.00854	0.02279	0.02127	0.01892	0.01807	0.01811	0.01901	0.02141	0.02296	0.00865
	1,536	T12	0.00814	0.01337	0.01237	0.01145	0.01114	0.01116	0.01152	0.01248	0.01351	0.00824
	1,680	T13	0.00760	0.00494	0.00317	0.00209	0.00160	0.00162	0.00215	0.00325	0.00504	0.00769
	1,824	T14	0.00702	0.00744	0.00030	-0.00457	-0.00663	-0.00661	-0.00451	0.00040	0.00753	0.00710
	1,968	T15	0.00628	0.01154	-0.00128	-0.01060	-0.01442	-0.01441	-0.01054	-0.00118	0.01164	0.00635
	2,112	T16	0.00545	0.00891	-0.00568	-0.01609	-0.02041	-0.02040	-0.01607	-0.00562	0.00899	0.00551
	2,256	T17	0.00453	0.00138	-0.00922	-0.01632	-0.01942	-0.01943	-0.01633	-0.00922	0.00142	0.00458
	2,400	T18	0.00346	0.00033	-0.00186	-0.00329	-0.00398	-0.00398	-0.00328	-0.00185	0.00034	0.00350
	2,520	T19	0.00269	0.00991	0.01351	0.01557	0.01645	0.01648	0.01564	0.01362	0.01000	0.00271
	2,640	T20	0.00155	0.02803	0.03830	0.04335	0.04547	0.04553	0.04354	0.03858	0.02830	0.00156

(c) Plate initial deflection for a = 6,300 ~ 9,650 mm (z-direction)

Plate initial deflections (w_0 / t_p)			Longitudinal direction (a = 6,300 ~ 9,650 mm)									
			6,300	6,650	7,000	7,350	7,700	8,050	8,400	8,750	9,100	9,450
			L19	L20	L21	L22	L23	L24	L25	L26	L27	L28
Transverse direction (b = 0 ~ 2,640 mm)	0	T1	0.00312	0.01575	0.01519	0.01988	0.02379	0.02535	0.02444	0.02177	0.01510	-0.00034
	120	T2	0.00527	0.01196	0.01469	0.01919	0.02250	0.02387	0.02292	0.01949	0.01251	-0.00076
	240	T3	0.00626	0.01069	0.01499	0.01866	0.02136	0.02260	0.02180	0.01828	0.01115	-0.00120
	384	T4	0.00729	0.01737	0.01817	0.01856	0.02014	0.02124	0.02106	0.01924	0.01247	-0.00161
	528	T5	0.00803	0.02612	0.02210	0.01904	0.01968	0.02067	0.02110	0.02132	0.01531	-0.00207
	672	T6	0.00856	0.02698	0.02213	0.01912	0.01983	0.02078	0.02106	0.02121	0.01551	-0.00248
	816	T7	0.00891	0.01910	0.01842	0.01903	0.02079	0.02172	0.02107	0.01882	0.01230	-0.00285
	960	T8	0.00907	0.01293	0.01722	0.02101	0.02357	0.02430	0.02265	0.01811	0.00995	-0.00320
	1,104	T9	0.00907	0.01949	0.02385	0.02700	0.02901	0.02912	0.02696	0.02242	0.01267	-0.00330
	1,248	T10	0.00892	0.02844	0.03166	0.03286	0.03386	0.03334	0.03106	0.02744	0.01673	-0.00338
	1,392	T11	0.00865	0.02858	0.03168	0.03289	0.03391	0.03339	0.03108	0.02746	0.01685	-0.00339
	1,536	T12	0.00824	0.01945	0.02357	0.02668	0.02875	0.02891	0.02676	0.02225	0.01274	-0.00333
	1,680	T13	0.00769	0.01159	0.01579	0.01953	0.02216	0.02305	0.02164	0.01738	0.00955	-0.00325
	1,824	T14	0.00710	0.01491	0.01473	0.01556	0.01733	0.01860	0.01871	0.01741	0.01152	-0.00291
	1,968	T15	0.00635	0.01998	0.01508	0.01240	0.01317	0.01481	0.01659	0.01864	0.01439	-0.00255
	2,112	T16	0.00551	0.01805	0.01210	0.00905	0.00998	0.01211	0.01461	0.01743	0.01377	-0.00213
	2,256	T17	0.00458	0.01049	0.00849	0.00874	0.01096	0.01336	0.01507	0.01547	0.01083	-0.00166
	2,400	T18	0.00350	0.00808	0.01303	0.01758	0.02109	0.02290	0.02236	0.01881	0.01141	-0.00122
	2,520	T19	0.00271	0.01595	0.02487	0.03114	0.03462	0.03519	0.03247	0.02634	0.01671	-0.00077
	2,640	T20	0.00156	0.03174	0.04489	0.05176	0.05413	0.05256	0.04704	0.03804	0.02571	-0.00034

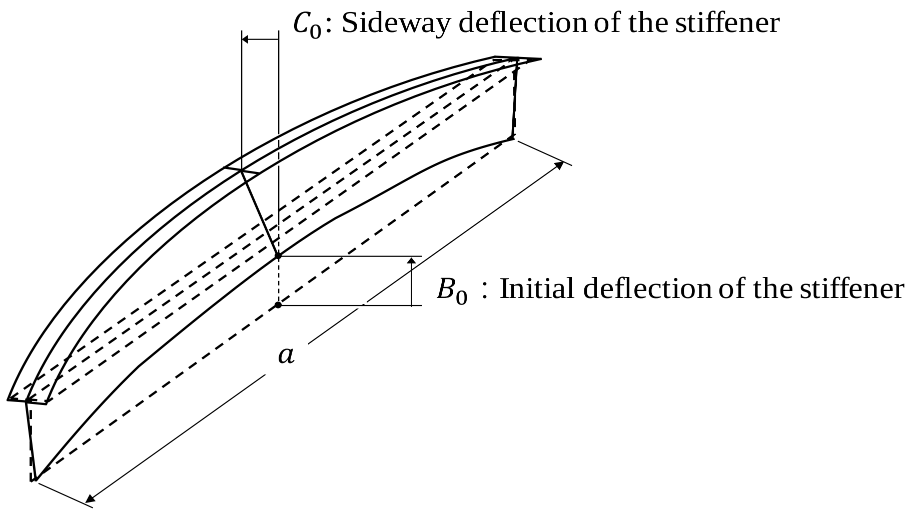

Fig. A.2. Definition of stiffener's deflections.

Table A2. Measured initial deflections of stiffeners normalized by stiffener thickness

(a) Initial deflection of the longitudinal stiffener (z-direction)

Stiffener initial deflections (w_0 / t_s)			Longitudinal direction (a = 0 ~ 3,150 mm)									
			0	350	700	1,050	1,400	1,750	2,100	2,450	2,800	3,150
			L1	L2	L3	L4	L5	L6	L7	L8	L9	L10
Transverse direction (b = 0 ~ 2,640 mm)	240	T3	0.00616	0.00367	0.00154	-0.00014	-0.00106	-0.00110	-0.00025	0.00140	0.00360	0.00626
	960	T8	0.00895	0.00682	0.00563	0.00500	0.00473	0.00473	0.00501	0.00566	0.00688	0.00907
	1,680	T13	0.00760	0.00494	0.00317	0.00209	0.00160	0.00162	0.00215	0.00325	0.00504	0.00769
	2,400	T18	0.00346	0.00033	-0.00186	-0.00329	-0.00398	-0.00398	-0.00328	-0.00185	0.00034	0.00350

Stiffener initial deflections (w_0 / t_s)			Longitudinal direction (a = 3,150 ~ 6,300 mm)									
			3,150	3,500	3,850	4,200	4,550	4,900	5,250	5,600	5,950	6,300
			L10	L11	L12	L13	L14	L15	L16	L17	L18	L19
Transverse direction (b = 0 ~ 2,640 mm)	240	T3	0.00616	0.00367	0.00154	-0.00014	-0.00106	-0.00110	-0.00025	0.00140	0.00360	0.00626
	960	T8	0.00895	0.00682	0.00563	0.00500	0.00473	0.00473	0.00501	0.00566	0.00688	0.00907
	1,680	T13	0.00760	0.00494	0.00317	0.00209	0.00160	0.00162	0.00215	0.00325	0.00504	0.00769
	2,400	T18	0.00346	0.00033	-0.00186	-0.00329	-0.00398	-0.00398	-0.00328	-0.00185	0.00034	0.00350

Stiffener initial deflections (w_0 / t_s)			Longitudinal direction (a = 6,300 ~ 9,650 mm)									
			6,300	6,650	7,000	7,350	7,700	8,050	8,400	8,750	9,100	9,450
			L19	L20	L21	L22	L23	L24	L25	L26	L27	L28
Transverse direction (b = 0 ~ 2,640 mm)	240	T3	0.00626	0.01069	0.01499	0.01866	0.02136	0.02260	0.02180	0.01828	0.01115	-0.00120
	960	T8	0.00907	0.01293	0.01722	0.02101	0.02357	0.02430	0.02265	0.01811	0.00995	-0.00320
	1,680	T13	0.00769	0.01159	0.01579	0.01953	0.02216	0.02305	0.02164	0.01738	0.00955	-0.00325
	2,400	T18	0.00350	0.00808	0.01303	0.01758	0.02109	0.02290	0.02236	0.01881	0.01141	-0.00122

(b) Initial deflection of the transverse stiffener (z-direction)

Stiffener initial deflections (w_0 / t_s)			Transverse direction (b = 0 ~ 1,248 mm)									
			0	120	240	384	528	672	816	960	1,104	1,248
			T1	T2	T3	T4	T5	T6	T7	T8	T9	T10
Longitudinal direction (a = 0 ~ 9,650 mm)	0	L10	0.00307	0.00519	0.00616	0.00719	0.00792	0.00845	0.00879	0.00895	0.00895	0.00881
	120	L19	0.00312	0.00527	0.00626	0.00729	0.00803	0.00856	0.00891	0.00907	0.00907	0.00892

Stiffener initial deflections (w_0 / t_s)			Transverse direction (b = 1,392 ~ 2,640 mm)									
			1,392	1,536	1,680	1,824	1,968	2,112	2,256	2,400	2,520	2,640
			T11	T12	T13	T14	T15	T16	T17	T18	T19	T20
Longitudinal direction (a = 0 ~ 9,650 mm)	0	L10	0.00854	0.00814	0.0076	0.00702	0.00628	0.00545	0.00453	0.00346	0.00269	0.00155
	120	L19	0.00865	0.00824	0.00769	0.0071	0.00635	0.00551	0.00458	0.0035	0.00271	0.00156

(c) Sideway initial deflection of the longitudinal stiffener (y-direction)

Stiffener sideway deflections (w_0 / t_s)			Longitudinal direction (a = 0 ~ 3,150 mm)									
			0	350	700	1,050	1,400	1,750	2,100	2,450	2,800	3,150
			L1	L2	L3	L4	L5	L6	L7	L8	L9	L10
Transverse direction (b = 0 ~ 2,640 mm)	240	T3	-0.00046	-0.00032	-0.00016	0.00016	0.00056	0.00087	0.00106	0.00128	0.00171	0.00429
	960	T8	-0.00055	-0.00111	-0.00220	-0.00319	-0.00367	-0.00340	-0.00229	-0.00058	0.00110	0.00363
	1,680	T13	-0.00067	0.00018	0.00165	0.00316	0.00426	0.00465	0.00422	0.00311	0.00188	0.00307
	2,400	T18	-0.00074	-0.00303	-0.00680	-0.01042	-0.01262	-0.01258	-0.00997	-0.00530	-0.00039	0.00289

Stiffener sideway deflections (w_0 / t_s)			Longitudinal direction (a = 3,150 ~ 6,300 mm)									
			3,150	3,500	3,850	4,200	4,550	4,900	5,250	5,600	5,950	6,300
			L10	L11	L12	L13	L14	L15	L16	L17	L18	L19
Transverse direction (b = 0 ~ 2,640 mm)	240	T3	0.00429	0.00424	0.00444	0.00525	0.00597	0.00598	0.00528	0.00448	0.00429	0.00438
	960	T8	0.00363	0.00172	-0.00218	-0.00601	-0.00826	-0.00826	-0.00599	-0.00215	0.00179	0.00372
	1,680	T13	0.00307	0.00598	0.01081	0.01526	0.01784	0.01784	0.01528	0.01083	0.00602	0.00316
	2,400	T18	0.00289	-0.00552	-0.02028	-0.03395	-0.04184	-0.04184	-0.03394	-0.02024	-0.00545	0.00295

Stiffener sideway deflections (w_0 / t_s)			Longitudinal direction (a = 6,300 ~ 9,650 mm)									
			6,300	6,650	7,000	7,350	7,700	8,050	8,400	8,750	9,100	9,450
			L19	L20	L21	L22	L23	L24	L25	L26	L27	L28
Transverse direction (b = 0 ~ 2,640 mm)	240	T3	0.00438	0.00180	0.00143	0.00128	0.00113	0.00081	0.00038	-0.00001	-0.00027	-0.00055
	960	T8	0.00372	0.00116	-0.00051	-0.00219	-0.00326	-0.00350	-0.00300	-0.00205	-0.00108	-0.00063
	1,680	T13	0.00316	0.00197	0.00326	0.00441	0.00486	0.00443	0.00327	0.00169	0.00016	-0.00074
	2,400	T18	0.00295	-0.00041	-0.00536	-0.01002	-0.01257	-0.01253	-0.01030	-0.00677	-0.00312	-0.00080

(d) Sideway initial deflection of the transverse stiffener (x-direction)

Stiffener sideway deflections (w_0 / t_s)			Transverse direction (a = 0 ~ 2,640 mm)									
			0	120	240	384	528	672	816	960	1,104	1,248
			T1	T2	T3	T4	T5	T6	T7	T8	T9	T10
Longitudinal direction (a = 0 ~ 9,650 mm)	3150	L10	-0.01591	-0.01593	-0.01595	-0.01598	-0.01600	-0.01602	-0.01604	-0.01605	-0.01605	-0.01604
	6300	L19	-0.04533	-0.04528	-0.04523	-0.04516	-0.04509	-0.04503	-0.04497	-0.04491	-0.04487	-0.04484

Stiffener sideway deflections (w_0 / t_s)			Transverse direction (a = 0 ~ 2,640 mm)									
			1,392	1,536	1,680	1,824	1,968	2,112	2,256	2,400	2,520	2,640
			T11	T12	T13	T14	T15	T16	T17	T18	T19	T20
Longitudinal direction (a = 0 ~ 9,650 mm)	3150	L10	-0.01603	-0.01601	-0.01598	-0.01595	-0.01591	-0.01585	-0.01579	-0.01572	-0.01568	-0.01563
	6300	L19	-0.04481	-0.04479	-0.04478	-0.04478	-0.04479	-0.04481	-0.04484	-0.04487	-0.04490	-0.04493